

## Measurement of anisotropic Brownian motion near an interface by evanescent light-scattering spectroscopy

M. Hosoda, K. Sakai, and K. Takagi

*Institute of Industrial Science, University of Tokyo, Roppongi 7, Minato-ku, Tokyo 106, Japan*

(Received 3 June 1998)

We performed a dynamic evanescent light-scattering experiment to observe the Brownian motion of the sphere particles near the solid-liquid interface. An evanescent wave generated in a colloidal solution picks up information on the dynamics close to the solid interface within the submicrometer penetration depth. Measurement was made for various diameters of polystyrene spheres in a wide wave-number range of light scattering. The autocorrelation function obtained for particles smaller than the penetration length shows nonexponential behavior, which is successfully described by considering the complex scattering wave number brought about by the finite interaction region between the light and the sphere. The diffusion constant near the interface is smaller than that for free diffusion in a bulk solution, suggesting the suppression of Brownian motion due to the hydrodynamic interaction between the sphere and the solid wall. Furthermore, the Brownian motion was found to be anisotropic with respect to the directions parallel and perpendicular to the interface. The two different diffusion constants can be obtained uniquely by observation over a wide range of wave number. The diffusion constants thus obtained agree well with the values derived from hydrodynamic theory.

[S1063-651X(98)11911-6]

PACS number(s): 68.45.-v, 05.40.+j

### I. INTRODUCTION

Local structure and properties of fluid materials in the vicinity of the solid substrate often differ from those in the bulk state due to the physical and chemical influence of the interface. Since these effects extend only of the order of a nanometer to a micrometer, observation of the near-interface region requires very sophisticated techniques to obtain information within such a thin layer. Recently, the evanescent wave has attracted a great deal of interest as a probe with high spatial resolution because of its strong localization to the interface. Especially for the investigation of the plane interface, the known decay profile of the evanescent wave gives a quantitative measure accurate to nanometers [1-3].

Of the various evanescent techniques, dynamic light scattering employing the evanescent wave as a light source is an effective method by which to study the mechanical properties in an interface region [4]. Thermal fluctuation of the density causes local spatial modulation of the optical index, which scatters the light. The scattering angle determines the size of the fluctuation to be observed and the temporal behavior of the fluctuation is studied by the spectroscopic analysis of the scattered light. The Brownian motion of small particles can also be observed by this technique. Observation of the Brownian motion enables us to study local dynamic properties of the materials, such as viscosity or elasticity. Up to now, this technique has been applied to observe the Brownian motion of sphere particles [4,5], concentration fluctuation of liposomes [6], or orientational fluctuation of liquid crystals [7], in which the motion was found to slow down due to the effect of the interface. In addition, anisotropic properties with respect to the direction of the interface plane, normal or parallel, have been suggested.

We performed an observation of the Brownian motion of sphere particles very close to the solid interface. The aniso-

tropic diffusion was successfully observed and the results were well explained by hydrodynamic analysis for the effective diffusion constant near the interface.

### II. DYNAMIC EVANESCENT LIGHT SCATTERING

An evanescent wave is a light field leaked into the medium with a lower index and localized within the depth of the order of the optical wavelength from the interface. When the light is incident to the interface from the optically dense solid to the sparse liquid at the incident angle  $\theta$  larger than the critical angle  $\theta_c$  [ $=\sin^{-1}(n_2/n_1)$ ], the light is totally reflected at the interface. Here,  $n_i$  is the index of the materials ( $n_1 > n_2$ ). The electric field generated in the liquid medium is described as

$$E(x, z) = E_0 \exp\{i(\omega t - Kx)\} \exp(-z/\xi), \quad (1)$$

where the interface and the incident planes are in the  $x$ - $y$  and  $x$ - $z$  planes, respectively. The electric field propagates as the sinusoidal wave along the interface with the wave number  $K = n_1 k_0 \sin \theta$ ,  $k_0$  being the optical wave number in a vacuum. The electric field is localized near the interface in the penetration length given by [8]

$$\xi = (n_1 k_0)^{-1} (\sin^2 \theta - \sin^2 \theta_c)^{-1/2}. \quad (2)$$

When the liquid medium is optically homogeneous, all the energy of light is reflected at the interface. If some inhomogeneity appears in the medium due to the thermal fluctuation of density or the existence of scatterers, the total reflection is frustrated. The evanescent wave is partially converted to the usual propagating light carrying energy. Here we consider the evanescent light scattering by small particles. The light scattered into the angle  $\varphi$  is written as

$$I = |E_0 \Sigma \exp(-i\omega t) \exp(ik_x x_i) \exp\{(ik_z - 1/\xi)z_i\}|^2, \quad (3)$$

where  $\mathbf{r}_i = (x_i, z_i)$  represents the position of the center of the  $i$ th particle, and  $k_x = K + n_2 k_0 \sin \varphi$  and  $k_z = n_2 k_0 \cos \varphi$  are the  $x$  and  $z$  components of the scattering wave vector  $\mathbf{k}$ , respectively.

In the usual light-scattering experiment performed for the bulk sample, the laser beam diameter is satisfactorily large and the scattering volume is regarded as infinite. This fact corroborates the condition that the scattering wave vector has a unique and real value. As for the evanescent light scattering, on the other hand, the interaction region between the particle and the light is limited by the finite penetration length  $\xi$ . The scattering wave number along the  $z$  direction appearing in Eq. (3) is, therefore, represented as the complex value,

$$k_z^* = k_z + i/\xi. \quad (4)$$

Fourier transformation of Eq. (4) into the wave-number space gives the spatial power spectrum of the structure to be observed experimentally as

$$S(k) \propto \frac{1}{(k - k_z)^2 + 1/\xi^2}. \quad (5)$$

This spectrum is a Lorentzian curve centering at  $k_z$  with the width of  $1/\xi$ .

Autocorrelation function of the intensity of the scattered light defined by  $g_2(t) = \langle I(t)I(0) \rangle$  gives information on the temporal behavior of the Brownian particles. For the particles in a free space, the correlation function shows single exponential decay written as  $\exp(-\Gamma t)$ , where the decay constant  $\Gamma$  is related to the scattering wave number  $k$  and the diffusion constant  $D$  by  $\Gamma = 2Dk^2$  in the homodyne detection. As will be described in the next section, the Brownian motion of particles near the liquid-solid interface is a complex phenomenon and the diffusion constant generally depends on the spacing distance between the particle and the interface. For simplification, we assume here that the diffusion constant is independent of the particle position. The correlation function is then given by the integral of the single exponential decay with weighting of Eq. (5) as

$$g_2(t, D_x, D_z) \propto \exp(-2D_x k_x^2 t) \int S(k) \exp(-2D_z k_z^2 t) dk. \quad (6)$$

Here, the diffusion is anisotropic as described later in detail and appropriate diffusion constants for the  $x$  and  $z$  directions are represented by  $D_x$  and  $D_z$ , respectively. The correlation function is not a single exponent any more but has a distribution of the decay time. The result obtained here is the same in principle as that given by the more rigorous calculation of the correlation function. Note again that the correlation function of Eq. (6) is given under the simple assumption that the diffusion constant does not depend on the position of the particle. As described later in detail, this assumption is not necessarily correct for some cases with small particles. The effect of the position-dependent diffusion is approximately taken into account in the following section.

### III. BROWNIAN MOTION OF SPHERE PARTICLES NEAR THE SOLID-LIQUID INTERFACE

A number of experimental results as well as theoretical approaches have been reported for the Brownian motion of a sphere particle close to a solid surface [5,9,10]. Brownian motion is a random walk of the particle in liquid driven by the thermal energy. The ensemble of particles with no interaction in between shows a diffusive behavior, the time constant of which is determined by the microscopic force of molecular collisions and the macroscopic quantity of hydrodynamics. Measurement of the diffusion constant gives information about the local mechanical properties of the surrounding material. A small sphere with a well determined diameter would be a good tracer to investigate the shear viscosity of the material.

As for the particle near the plane wall, we expect that the Brownian motion would be suppressed due to hydrodynamic interaction between the sphere and the wall. It is also predicted that the diffusion would be anisotropic along the  $x$  and  $z$  directions. The effective diffusion constants are given by [10]

$$D_x = (1 + s/a)/(25/16 + s/a) D_{\text{bulk}},$$

$$D_z = \left[ \frac{4}{3} \sinh \alpha \sum_{m=1}^{\infty} \frac{m(m+1)}{(2m-1)(2m+3)} \left\{ \frac{2 \sinh(2m+1)\alpha + (2m+1) \sinh 2\alpha}{4 \sinh^2(m+1/2)\alpha - (2m+1)^2 \sinh^2 \alpha} - 1 \right\} \right]^{-1} D_{\text{bulk}}, \quad (7)$$

where  $\alpha = \cosh^{-1}(1+s/a)$ ,  $s$  being the spacing distance between the particle and interface, and  $D_{\text{bulk}}$  is the diffusion constant in a free space. Figure 1 shows the numerical solution of Eq. (7) given as the ratio of  $D_x$  or  $D_z$  to  $D_{\text{bulk}}$ . The evanescent wave has a finite penetration length  $\xi$ , which limits the distance between the wall and the particles contributing to the light scattering. For particles whose diameter is smaller than  $\xi$ , the factor  $s/a$  ranges from zero to a value larger than unity, while it is safely regarded as zero for particles much larger than  $\xi$ . The Brownian motion would show

different behavior near the interface since the effective diffusion constant, especially that for the vertical motion, drastically changes with the gap in the region of  $0 < s/a < 1$  as shown in Fig. 1.

Here we describe the relation between the particle size and the Brownian behavior expected from the hydrodynamic theory. We have to pay attention to the distribution of particles along the direction of gravity. When the solid surface is set horizontally, particles distribute with profiles determined by the potential near the interface formed by, for ex-

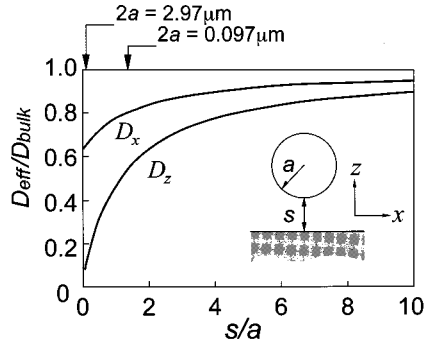


FIG. 1. Anisotropic diffusion constants of sphere particles near the liquid-solid interface calculated with the hydrodynamic theory. The ordinate represents the ratio of the effective diffusion constant to that in bulk, while the abscissa shows the distance between the particle and the interface normalized by the sphere radius. The subscripts  $x$  and  $z$  show the direction of motion as indicated in the figure.

ample, gravitational and electrical effects. It is known that an electric double layer exerts repulsive force between a sphere and a glass plate, which prevents their intimate contact. This effect makes a short-range interaction, however, and we neglect it in the following discussion. Considering the gravitational potential, distribution of the particles is given by

$$N(s) = N_0 \exp\left(-\frac{4\pi a^3 \Delta \rho g s}{3k_B T}\right), \quad (8)$$

where  $\Delta \rho$  is the difference in density between the particle and the surrounding liquid,  $N_0$  is a constant,  $T$  is the temperature, and  $g$  and  $k_B$  are the gravitational and Boltzmann constants, respectively. Roughly estimating, the particles distribute above the interface within the localization thickness of  $h = 3k_B T / 4\pi a^3 \Delta \rho g$ . We found three parameters  $a$ ,  $\xi$ , and  $h$  characterizing the Brownian behavior, which is roughly classified into two typical cases.

#### A. Particles smaller than the evanescent penetration length, i.e., $2a < \xi$

Through light scattering one observes a diffusion process of particles with different diffusion constants dependent on each gap distance. Though the analysis of the exact correlation function in the present case is somewhat difficult, it is possible to make an approximation stating that the correlation function is obtained by the integral over the distributing diffusion constant for the early behavior. We should also consider the distribution of the wave number brought about by the finite interaction length along the  $z$  axis, which was described in the preceding section. The final form of the correlation function is then given with  $g_2(t)$  of Eq. (6) as

$$G(t) \propto \int g_2\{t, D_x(s), D_z(s)\} \exp(-s/\xi) N(s) ds. \quad (9)$$

Here the effect of the position-dependent diffusion constants is approximately taken into account by replacing the diffusion constant in Eq. (6) by the value averaged with respect to the spacing distance  $s$ . This equation provides a correct description of the behavior at least in the initial stage.

As for the polystyrene particles,  $2a < 0.1 \mu\text{m}$  corresponds with the present condition.

#### B. Particles larger than the evanescent penetration length, i.e., $2a > \xi$

We observe light scattering from particles whose bottom is close to the solid surface within its diameter. The Brownian motion slows down and the diffusion constant becomes smaller for both the  $x$  and  $z$  directions. As shown in Fig. 1, the diffusion constant for the vertical direction is smaller than one-tenth of the value in bulk at  $s/a = 0.1$ . The vertical diffusion is almost frozen and we can neglect the motion along the  $z$  axis. For the  $x$  direction, on the other hand, the diffusion constant takes a finite value at  $s/a = 0$ . The hydrodynamic theory predicts  $(16/25)D_{\text{bulk}}$  as the limiting value of the horizontal diffusion constant. In this case, only the diffusion along the  $x$  direction causes the temporal fluctuation of the scattered light intensity. We do not have to pay attention to the complex  $z$  component of the scattering wave number, and the correlation function is given in a single exponential form  $G(t) = \exp(-2D_x k_x^2 t)$ . The corresponding particle diameter is  $2a > 0.5 \mu\text{m}$ .

In addition to the above two cases, we should consider the special case in which the particle is large enough and  $h$  is smaller than  $2a$ . When the particle is larger than  $10 \mu\text{m}$ , gravity presses the particle downward within a height shorter than its diameter. The particles do not touch the wall, however, because of the electric repulsive force. They stay around the bottom of the potential well and cannot move along the  $z$  direction, overcoming the potential barrier. The particles show the vertical Brownian motion in the potential well. Though the position of each particle fluctuates, the time constant is not the function of the scattering wave number any more, but is determined as the ratio of the restoring force and dissipation strength. Also in this case, the effective viscosity against the vertical motion is much larger than that in a free space, and we can neglect diffusion in the  $z$  direction.

## IV. EXPERIMENT

We made both evanescent light scattering and conventional dynamic light scattering experiments to observe the Brownian motion of small particles dispersed in water just close to the solid interface and in a bulk state. A block diagram of the dynamic evanescent light-scattering system is shown in Fig. 2. The light source is a frequency doubled YAG (yttrium aluminum garnet) laser with a wavelength of 532 nm and an output power of 400 mW. The sample liquid is put on the top surface of a  $45^\circ$  right angle prism.

The laser beam is incident to the prism from the oblique plane at  $56^\circ$ , the Brewster angle of the air-glass interface. In this geometry, the light reflected twice within the prism comes back to the incident face at the Brewster angle and exits the prism leaving no stray light. The evanescent scattering is very weak and the exclusion of the stray light is an essential technique for sensitive measurement. A prism made of glass with an index 1.5 has a critical angle  $62.5^\circ$ . The beam is totally reflected at the top surface of the prism at an angle of  $78^\circ$ . The evanescent wave is generated in the liquid sample and propagates along the interface with a wave number  $K = 1.736 \times 10^7 \text{ m}^{-1}$ . The penetration length is calcu-

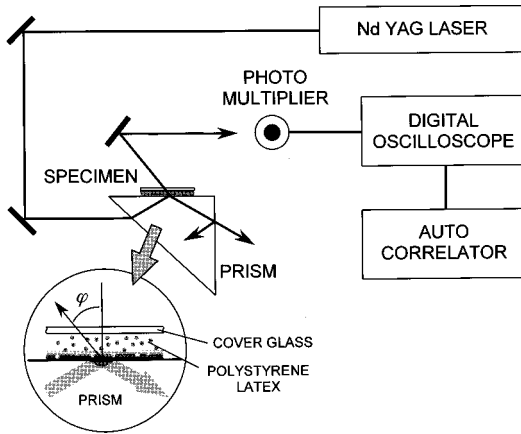


FIG. 2. Block diagram of the experimental system.

lated to be  $\xi = 140$  nm from Eq. (2) for the present angle of incidence.

The sample is polystyrene latex, an aqueous dispersion of polystyrene spheres whose diameter is well determined. The sample is spread on the prism with a thickness of 0.5 mm and covered with a thin glass plate. Diameters of the polystyrene spheres used are 0.097, 0.813, 2.97, and 11.9  $\mu\text{m}$ . The localization depths are calculated from Eq. (8) with a density of polystyrene of  $\Delta\rho = 1.05$  g/cm<sup>3</sup> to  $h = 5.5$  cm, 70  $\mu\text{m}$ , 2  $\mu\text{m}$ , and 30 nm, respectively. The concentration of each sample is determined considering these localization depths so as to keep the distance to the nearest neighbor more than ten times larger than the diameter. Therefore, the interaction between particles can be ignored and we consider only the hydrodynamic effect between a lone particle and a plane wall. The sample is almost transparent and the light penetrates through it without serious intensity loss. Only the particles very close to the surface scatter the evanescent wave, which is converted to the normal propagating light. When the scattering angle  $\varphi$  is larger than 50°, another prism is attached in contact with the glass cover to prevent the total reflection of the scattered light at the glass-air interface and to pick up the scattered light. The wave number of the measurement ranges from  $k = 1.6 \times 10^6$  m<sup>-1</sup> to  $3.3 \times 10^7$  m<sup>-1</sup>.

A He-Ne laser is used as a guide beam for accurate determination of the scattering angle. The He-Ne laser crosses the YAG laser just at the scattering point on the prism surface, and the position of the photodetector is adjusted so that its surface neatly accepts the guide laser beam coming out of the prism. The detector is a photomultiplier whose output current is sent to the digital oscilloscope, and the autocorrelation function of the signal is calculated by a computer.

## V. RESULTS AND DISCUSSIONS

### A. Examination of the nonexponential correlation function

As described in the preceding section, the correlation function of scattered light intensity is expected to show nonexponential behavior and its form might give information on the anisotropic diffusion of Brownian particles near the interface. The typical correlation function obtained is shown in Fig. 3 for (a) the particle diameter  $2a = 0.097$   $\mu\text{m}$  at the scattering angle  $\varphi = -61^\circ$  and (b)  $2a = 2.97$   $\mu\text{m}$  at  $\varphi = -21^\circ$ . Apparently, the correlation function in (a) deviates

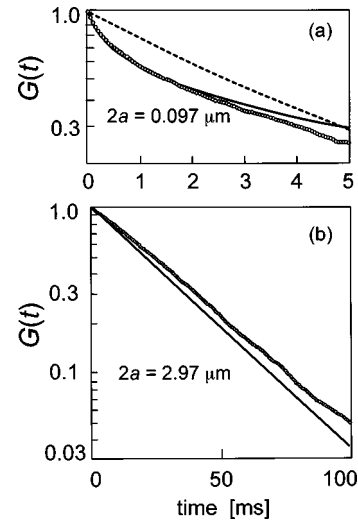


FIG. 3. Normalized autocorrelation function of the scattered light intensity observed for the polystyrene latex with a particle diameter of (a)  $2a = 0.097$   $\mu\text{m}$  at the scattering angle of  $\varphi = -61^\circ$  and (b)  $2a = 2.97$   $\mu\text{m}$  at  $\varphi = -21^\circ$ . The solid line in each figure shows the theoretical reproduction of the correlation function obtained taking into account the effects of both the distributions in the vertical wave number and the diffusion constant. The dashed line shows the theoretical curve obtained without the effect of the distributed wave number.

from the straight line and shows nonexponential behavior. The major reasons for this nonexponential correlation function are the following: distribution in the wave number  $k_z$ , the gap-dependent diffusion constant, and the fluctuation of the total number of particles in the scattering volume. In the early stage of correlation, i.e.,  $(D_z t)^{1/2} < \xi$ , the population fluctuation could be ignored. This assumption holds at  $t < 5$  ms in the present case. The dashed line in Fig. 3(a) is the theoretical curve of the correlation function calculated considering only the effect of the gap-dependent diffusion constant. Actually, the autocorrelation function is calculated from the rigorous expression of Eq. (9) with a unique value of  $k_z$ , namely  $S(k) = \delta(k_z)$  in Eq. (5). The theoretical curve thus obtained does not reproduce the experimental data as shown in the figure.

Then we take into account also the distribution of the wave number  $k_z$  and obtain the theoretical curve with Eq. (9), which is shown by the solid line. The experimental data agree well with this theoretical curve. All the quantities used for the calculation are found in the preceding sections including the distribution of the wave number and the diffusion constant. We found that nonexponential behavior of the autocorrelation function is mainly derived from the distribution of the perpendicular component of the scattering vector. As far as only the early stage of the correlation is concerned, we can successfully reproduce the experimental result analytically without introducing any fitting parameters.

For the particles whose diameter is much larger than the evanescent penetration length, i.e.,  $2a \gg \xi$ , the condition  $s/a \ll 1$  holds and the effective diffusion constant along the  $z$  axis becomes negligibly small compared to the value at far from the interface, as shown in Fig. 1. On the other hand, another diffusion constant along the  $x$  axis approaches a constant value as also shown in the figure. As for the particle

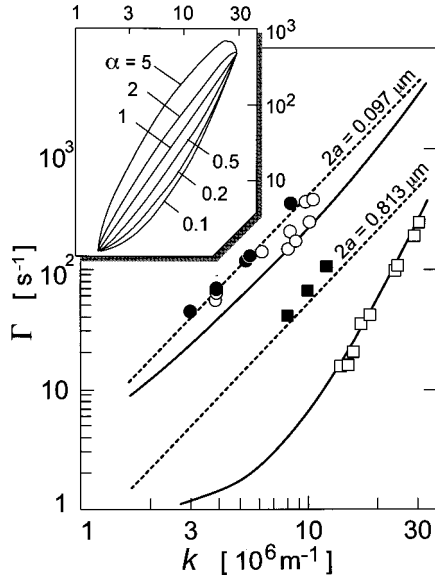


FIG. 4. Temporal decay constant plotted against the scattering wave number  $k$ , obtained for the particle diameters of  $0.097 \mu\text{m}$  (circles) and  $0.813 \mu\text{m}$  (squares). Open and closed symbols show the values near the interface and in bulk, respectively. The dashed lines show the theoretical behavior in bulk obtained with the diffusion constant given by the Stokes-Einstein relation. The solid lines are the theoretical prediction for anisotropic diffusion near the interface derived from Eq. (10). The inset shows the  $\alpha$  dependence of the  $\Gamma$ - $k$  relation calculated for the particle diameter of  $0.813 \mu\text{m}$ .

with  $2a=2.97 \mu\text{m}$ , the factor  $s/a$  is regarded as zero and  $D_x=(16/25)D_{\text{bulk}}$  and  $D_z=0$  are good approximations, though the ambiguity remains in determining  $k_z$ . It would not matter, however, since the diffusion perpendicular to the interface is almost frozen and only the parallel motion of the particle contributes to the fluctuation of the scattered light intensity. The correlation function shown in Fig. 3(b) shows single exponential behavior. The solid line shows the theoretical curve obtained from Eq. (6) with the known values of  $D_x=(16/25)D_{\text{bulk}}$  and  $D_z=0$ . It explains well the actual behavior of the correlation function. Correlation functions observed for particles with diameters of  $0.813$  and  $11.9 \mu\text{m}$  also show single exponential behavior. The Brownian motion of the particles that are at least five times larger than the evanescent penetration length reflects the viscosity along and near the interface. The correlation form thus tells us whether the vertical motion is frozen or not.

### B. Anisotropic diffusion of sphere particles near the liquid-solid interface

As has been described in the preceding section, the relation between the decay constant and the scattering wave number would yield information on the anisotropy of the diffusion process. The autocorrelation function of the scattered light intensity was observed for various sphere diameters varying the scattering angle. The decay constant  $\Gamma$ , which is the inverse of the correlation time thus obtained, is plotted against  $k$  in Figs. 4 and 5 as open symbols. The abscissa indicates the scattering wave number given by  $k=(k_x^2+k_z^2)^{1/2}$ . The nonexponential correlation function such as that given in Fig. 3(a) would not give a unique value of  $\Gamma$ .

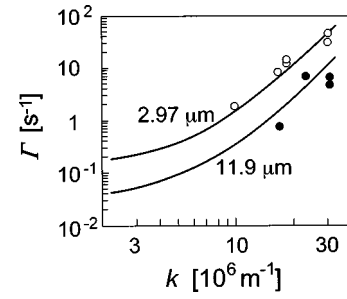


FIG. 5. Temporal decay obtained by the evanescent light scattering for the particle diameter of  $2.97 \mu\text{m}$  (open circles) and  $11.9 \mu\text{m}$  (closed circles). The solid lines are the theoretical prediction for the  $\Gamma$ - $k$  relation derived from Eq. (10) with the limiting values of anisotropic and suppression parameters at  $s \rightarrow 0$ , i.e.,  $\alpha=0$  and  $\sigma=0.64$ , respectively.

For convenience we determined  $\Gamma$  as the inverse of the time at which the normalized correlation function decays to  $1/e$ . As for the larger particles whose correlation function is a single exponent,  $\Gamma$  is obtained from the gradient of the semi-logarithmic plot of the correlation function. The closed circle is the decay constant experimentally obtained in the bulk state and the dashed lines show the theoretical prediction obtained with the diffusion constant in a free space given by the Stokes-Einstein relation for each diameter together with the known values of the viscosity. Note that the diffusive process through Brownian motion is characterized by the relation  $\Gamma=2Dk^2$ . The decay constants obtained by the evanescent light scattering are slightly smaller than the bulk value for  $0.097\text{-}\mu\text{m}$ -diam particles suggesting the slowing down of the Brownian motion near the interface. For  $0.813 \mu\text{m}$  diam, on the other hand, the decay constant at the interface is by far smaller than those in bulk and the gradient is larger than 2. Now we explain this strange behavior of the  $\Gamma$ - $k$  relation. The scattering vector has  $x$  and  $z$  components and their contribution changes depending on the scattering angle. At the experimental limits of  $\varphi=\pi/2$  and  $-\pi/2$ , the scattering vector is directed along the  $x$  axis and only the motion parallel to the interface is picked up by the light scattering. In the intermediate region, the scattering wave vector has  $z$  components and we observe also the motion perpendicular to the interface. If the particle is driven by the isotropic diffusion process as in the case of bulk, the dispersion relation would be a straight line with the gradient of 2. If the diffusion is anisotropic, i.e.,  $D_x \neq D_z$ , the dispersion relation would deviate from the straight line and its curvature would give information on the degree of the anisotropy. The curve is convex downward if the diffusion along the  $x$  direction is faster than that along the  $z$  direction, and vice versa if the latter is faster, though it would be a rare case.

For simplification we introduce two new parameters here: the anisotropic coefficient  $\alpha$  and the suppression coefficient  $\sigma$  as defined by  $\alpha=D_z/D_x$  and  $\sigma=D_x/D_{\text{bulk}}$ , respectively. The dispersion relation is uniquely determined with these two factors as

$$\Gamma = D_{\text{bulk}} \sigma (k_x^2 + \alpha k_z^2). \quad (10)$$

The expected  $\Gamma$ - $k$  relation for various values of  $\alpha$  is shown in the inset of Fig. 4. In addition, the suppression factor

makes a lateral shift to the dispersion curve. In principle, we can determine  $\alpha$  and  $\sigma$  and  $D_x$  and  $D_z$  uniquely by observing the whole aspect of the  $\Gamma$ - $k$  relation in a wide wave-number range. The solid lines in Fig. 4 are the theoretical prediction obtained with the known values of  $\alpha$  and  $\sigma$ :  $\alpha=0.64$  and  $\sigma=0.81$  for  $0.097 \mu\text{m}$  diam and  $\alpha=0$  and  $\sigma=\frac{16}{25}$  for  $0.813 \mu\text{m}$  diam. The values for  $0.097 \mu\text{m}$  are obtained by numerical averaging of the diffusion constant by taking into account the decay profile of the evanescent light. Note here again that no fitting parameter is employed to calculate these theoretical curves. As can be seen, they explain well the dispersion relation experimentally obtained. Figure 5 shows the dispersion relation obtained for larger particles with  $2a=2.97$  and  $11.9 \mu\text{m}$ . The vertical diffusion for these particles is suppressed not only by the hydrodynamic interaction with the interface, but also by the gravity. They stay close to the interface and we can completely ignore the effect of the  $z$  component in the scattering vector. The solid lines are the theoretical curve for the limiting condition of  $s/a=0$ . The remarkable agreement between the theoretical prediction and the experimental results naturally leads to the conclusion that the Brownian motion is anisotropic in the vicinity of a solid interface.

## VI. CONCLUSION

An evanescent light scattering experiment was performed to observe the Brownian motion of the sphere particles near the solid interface. The autocorrelation function reflecting the diffusion process of the small particles comparable to the evanescent penetration length shows nonexponential decay, which is reproduced by taking the distributions of the scattering wave number and the diffusion constant into consideration. The relation between the temporal decay constant of the correlation function and the wave number gives information on the anisotropy of the diffusion. Wide-band measurement may be able to determine uniquely the anisotropic diffusion constants. We are planning to apply the system for the measurement of anisotropic structure and viscoelastic properties of liquid crystals in the vicinity of the rubbed interface.

## ACKNOWLEDGMENT

This work was partially supported by a Grant-in-Aid for Scientific Research from the Ministry of Education, Science, Culture and Sports, Japan.

- 
- [1] Herman Chew, Dau-Sing Wang, and Milton Kerker, *Appl. Opt.* **18**, 2679 (1979).
  - [2] Scott G. Flicker and Stacy G. Bike, *Langmuir* **9**, 257 (1993).
  - [3] Binhua Lin and Stuart A. Rice, *J. Chem. Phys.* **99**, 8308 (1993).
  - [4] K. H. Lan, N. Ostrowsky, and D. Sornette, *Phys. Rev. Lett.* **57**, 17 (1986).
  - [5] N. Garnier and N. Ostrowsky, *J. Phys. II* **1**, 1221 (1991).
  - [6] A. K. Gaigalas, J. B. Hubbard, A. L. Plant, and V. Reipa, *J. Colloid Interface Sci.* **175**, 181 (1995).
  - [7] C. S. Park, M. Copic, R. Mahmood, and N. A. Clark, *Liq. Cryst.* **16**, 135 (1994).
  - [8] O. Bryngdahl, *Progress in Optics* (North-Holland, New York, 1983), Vol. 11.
  - [9] Laurent Lobry and Nicole Ostrowsky, *Phys. Rev. B* **53**, 12 050 (1996).
  - [10] Howard Brenner, *Chem. Eng. Sci.* **16**, 242 (1961).